

AN ANALYTICAL APPROACH TO ANALYZE NONLINEAR DYNAMIC RESPONSE OF ECCENTRICALLY STIFFENED FUNCTIONALLY GRADED CIRCULAR CYLINDRICAL SHELLS SUBJECTED TO TIME DEPENDENT AXIAL COMPRESSION AND EXTERNAL PRESSURE. PART 2: NUMERICAL RESULTS AND DISCUSSION

Dao Van Dung¹, Vu Hoai Nam²

¹*Hanoi University of Science, VNU, Viet Nam*

²*University of Transport Technology, Hanoi, Viet Nam*

*E-mail: hoainam.vu@utt.edu.vn

Received December 15, 2013

Abstract. Based on the classical thin shell theory with the geometrical nonlinearity in von Karman-Donnell sense, the smeared stiffener technique, Galerkin method and an approximate three-term solution of deflection taking into account the nonlinear buckling shape is chosen, the governing nonlinear dynamic equations of eccentrically stiffened functionally graded circular cylindrical shells subjected to time dependent axial compression and external pressure is established in part 1. In this study, the nonlinear dynamic responses are obtained by fourth order Runge-Kutta method and the nonlinear dynamic buckling behavior of stiffened functionally graded shells under linear-time loading is determined by according to Budiansky-Roth criterion. Numerical results are investigated to reveal effects of stiffener, input factors on the vibration and nonlinear dynamic buckling loads of stiffened functionally graded circular cylindrical shells

Keywords: Functionally graded material, discontinuous reinforcement, buckling, elasticity, analytical modelling.

1. INTRODUCTION

Governing equations of this problem are established in Part 1: “An analytical approach to analyze nonlinear dynamic response of eccentrically stiffened functionally graded circular cylindrical shells subjected to time dependent axial compression and external pressure. Part 1: Governing equations establishment” of the paper. In this part, effects of stiffener, material and geometric properties on the vibration and dynamic buckling behavior of cylindrical shells are numerically investigated.

Semi-analytical approach has become popular to investigate nonlinear dynamic response of mechanic structure analysis. Bich et al. [1–3] and Huang and Han [4] studied nonlinear dynamic buckling and vibration of FGM cylindrical shell, shallow double curved shell and cylindrical shell with and without stiffeners by using Runge-Kutta method. Due to linear deflection mode shape of solution, the dynamic responses of structures are obtained by solving one nonlinear second-order differential equation. The critical dynamic buckling is determined by applying Budiansky-Roth criterion [5] with only response of linear deflection term.

An approximate three-term solution of deflection taking into account the nonlinear buckling shape is chosen in Part 1. The obtained equations (36–38) are the nonlinear second-order differential three equations system. In this paper, this equation system is also solved by four order Runge-Kutta method. The vibration behavior of stiffened functionally graded circular cylindrical shells is carefully investigated and the dynamic critical time t_{cr} can be obtained according to Budiansky-Roth criterion [5] with total response of pre-buckling uniform, linear buckling, and nonlinear deflections. For large value of loading speed, the amplitude-time curve of obtained displacement response increases sharply depending on time and this curve obtain a maximum by passing from the slope point and at the corresponding time $t = t_{cr}$ the stability loss occurs. Here t_{cr} is called critical time and the load corresponding to this critical time is called dynamic critical buckling load. The results show the effects of stiffener, volume-fraction index and geometrical parameters on the dynamic behavior of shells.

2. NUMERICAL RESULTS AND DISCUSSIONS

2.1. Validation of the present approach

The natural frequencies with basic vibration mode in longitudinal direction $m = 1$ and various vibration modes in circumferential direction n of isotropic cylindrical shells reinforced by stringer stiffeners of present study are compared to ones of Sewall and Naumann [6] and Sewall et al. [7] which were used trigonometric functions for circumferential modes, beam vibration functions for longitudinal modes, Rayleigh-Ritz procedure [6, 7] and ignored stiffener eccentricities [7] in Figs. 1–3. The simply supported cylindrical shells are used in these comparisons have geometrical and material properties: $L = 60.96$ cm, $E = 68.95$ GN/cm², $\nu = 0.315$, $\rho = 2.7145 \times 10^3$ kg/m³, $s_s = 25.4$ mm.

The static buckling of stiffened isotropic cylindrical shells under external pressure were studied by Baruch and Singer [8], Reddy and Starnes [9] and Shen [10] (see Tab. 1) and the dynamic buckling of un-stiffened FGM cylindrical shells under axial compression is considered (see Tab. 2), which was also analyzed by Huang and Han [4] using the energy method, classical shell theory and linear buckling shape. As can be seen, the good agreements are obtained in these comparisons.

2.2. Dynamic responses of ES-FGM cylindrical shell

To illustrate the present approach, the FGM cylindrical shells are considered with $R = 0.5$ m, $L = 0.75$ m, $E_m = 7 \times 10^{10}$ N/m², $\rho_m = 2702$ kg/m³, $E_c = 38 \times 10^{10}$ N/m², $\rho_c = 3800$ kg/m³, $\nu = 0.3$, $h_s = h_r = 0.01$ m, $d_s = d_r = 0.0025$ m, $n_r = 15$ and $n_s = 63$.

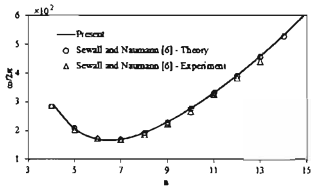


Fig. 1. Comparison of natural frequency of isotropic un-stiffened cylindrical shells ($R = 242.3$ mm, $h = 0.648$ mm)

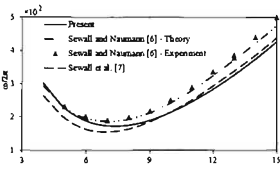


Fig. 2. Comparison of natural frequency of isotropic external stiffened cylindrical shells ($R = 242.2$ mm, $h = 0.650$ mm, $A_s = 18.92$ mm², $I_s = 0.034802$ cm⁴, $z_s = 3.655$ mm)

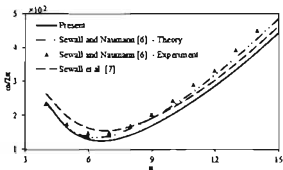


Fig. 3. Comparison of natural frequency of isotropic internal stiffened cylindrical shells ($R = 242.2$ mm, $h = 0.676$ mm, $A_s = 18.85$ mm², $I_s = 0.034641$ cm⁴, $z_s = 3.653$ mm)

Table 1. Comparisons of static buckling of internal stiffened isotropic cylindrical shells under external pressure (Psi)

	Baruch and Singer [8]	Reddy and Starnes [9]	Shen [10]	Present
Un-stiffened	102	93.5	100.7(4) ^a	103.327(4)
Stringer stiffened	103	94.7	102.2(4)	104.494(4)
Ring stiffened	370	357.5	368.3(3)	379.694(3)
Orthogonal stiffened	377	365	374.1(3)	387.192(3)

^a The numbers in the parenthesis denote the buckling modes (n), $m = 1$.

The material properties are $E_s = E_c$ and $E_r = E_c$, $\rho_s = \rho_c$ and $\rho_r = \rho_c$ with internal stringer stiffeners and internal ring stiffeners; $E_s = E_m$, $E_r = E_m$, $\rho_s = \rho_m$ and $\rho_r = \rho_m$ with external stringer stiffeners and external ring stiffeners, respectively.

Table 2. Comparisons of dynamic buckling of un-stiffened perfect FGM cylindrical shells under axial compression load (MPa)

	Present	Huang and Han [4]
$R/h = 500, L/R = 2, \xi_0 = 0, c = 100 \text{ MPa/s}$		
$k = 0.2$	195.74(2,11) ^b	194.94(2,11)
$k = 1.0$	170.69(2,11)	169.94(2,11)
$k = 5.0$	150.92(2,11)	150.25(2,11)
$R/h = 500, L/R = 2, \xi_0 = 0, k = 0.5$		
$c = 100 \text{ MPa/s}$	182.49(2,11)	181.67(2,11)
$c = 50 \text{ MPa/s}$	180.06(2,11)	179.37(2,11)
$c = 10 \text{ MPa/s}$	177.62(2,11)	177.97(1,8)
$L/R = 2, \xi_0 = 0, k = 0.2, c = 100 \text{ MPa/s}$		
$R/h = 800$	126.05(2,12)	124.91(2,12)
$R/h = 600$	163.37(3,14)	162.25(3,14)
$R/h = 400$	239.99(5,15)	239.18(5,15)

^b The numbers in the parenthesis denote the buckling modes (m, n) .

Table 3. Fundamental frequency (rad/s) of ES-FGM cylindrical shells

R/h	k	Un-stiffened	Internal stiffeners	External stiffeners
100	0.2	3070.77(6) ^c	3781.47(5)	3250.78(6)
	1	2597.44(6)	3412.62(5)	2894.66(5)
	5	2139.72(6)	2976.92(4)	2454.96(5)
	10	2020.20(6)	2784.62(4)	2318.83(5)
250	0.2	1963.37(8)	3530.27(5)	2647.36(6)
	1	1654.05(8)	3262.19(5)	2518.90(6)
	5	1364.74(7)	2728.48(4)	2211.58(5)
	10	1274.76(7)	2544.01(4)	2099.00(5)
400	0.2	1547.90(9)	3477.80(5)	2623.28(6)
	1	1305.02(9)	3153.82(4)	2492.46(5)
	5	1076.05(8)	2573.74(4)	2174.01(5)
	10	1005.85(8)	2399.42(4)	2073.93(5)

^c The numbers in the parenthesis denote the buckling modes $(n, m = 1)$.

The fundamental frequencies of natural vibration of ES-FGM cylindrical shells are shown in Tab. 3. As can be seen, the fundamental frequency of stiffened shells is larger than one of un-stiffened shells. The greatest is the fundamental frequency of internal stiffened shells. In addition, the fundamental frequency decreases when k increases. For example, $\omega_{mn} = 3781.47 \text{ rad/s}$ ($k = 0.2$) is larger than $\omega_{mn} = 2784.62 \text{ rad/s}$ ($k = 10$) about 1.36 times for $R/h = 100$ and internal stiffened shell. This property corresponds to the real

property of material because the higher value of k implies a metal-rich cylindrical shells which usually has lower stiffness than a ceramic-rich one.

Fig. 4 shows the effect of excitation force Q on the amplitude-frequency curves of nonlinear vibration of stiffened FGM cylindrical shell. As can be seen, when the excitation force decreases, the frequency-amplitude curves of forced vibration are closer to the amplitude-frequency curve of free vibration.

Fig. 5 investigates effect of R/h ratio on the frequency-amplitude curve of nonlinear free vibration. The obtained results show that the frequency-amplitude curve of thicker shell is lower than one of thinner shell.

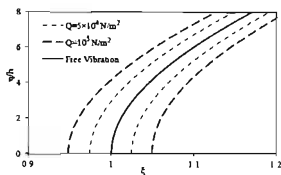


Fig. 4. The frequency-amplitude curve of nonlinear vibration of external stiffened FGM cylindrical shell ($R/h = 400$, $k = 1$, $m = 1$, $n = 5$)

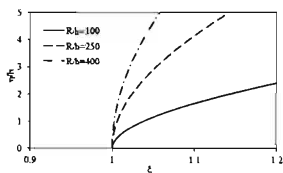


Fig. 5. The frequency-amplitude curve of nonlinear vibration of external stiffened FGM cylindrical shell ($k = 1$, $m = 1$, $n = 5$)

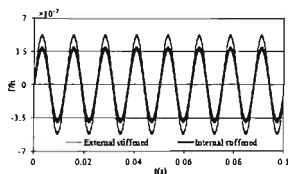


Fig. 6. Nonlinear dynamic responses of external and internal stiffened FGM cylindrical shells ($R/h = 250$, $k = 1$, $q(t) = 2 \times 10^5 \sin(500t)$)

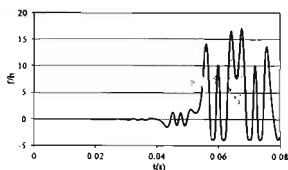


Fig. 7. Nonlinear dynamic responses of un-stiffened FGM cylindrical shells ($R/h = 250$, $k = 1$, $q(t) = 2 \times 10^5 \sin(500t)$)

Figs. 6 and 7 present the nonlinear responses of stiffened and un-stiffened FGM cylindrical shell with $R/h = 250$, $k = 1$. Fundamental frequency of un-stiffened and stiffened cylindrical shells are 1654.05 rad/s, 2518.90 rad/s (external stiffeners) and 3262.19 rad/s (internal stiffeners), respectively (see Tab. 3). The excitation frequencies are much smaller (Figs. 6 and 7, $q_0(t) = 2 \times 10^5 \sin(500t)$) than fundamental frequency. These results show that the stiffeners considerably decrease vibration amplitude when excitation frequencies are far from the fundamental frequency.

When the excitation frequencies are near to fundamental frequency, the interesting phenomenon is observed like the harmonic beat phenomenon of a linear vibration (Figs. 8 and 9). The excitation frequency is 2450 rad/s which is near to fundamental frequency 2518.90 rad/s of external stiffened cylindrical shell. The result shows that the amplitude of beats increases rapidly when the excitation frequency approaches the fundamental frequency.

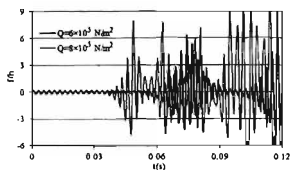
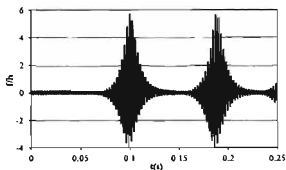


Fig. 8. Nonlinear dynamic responses of external stiffened FGM cylindrical shells ($R/h = 250, k = 1, q(t) = 5 \times 10^5 \sin(2450t), m = 1, n = 6$)

Fig. 9. Nonlinear dynamic responses of external stiffened FGM cylindrical shells ($R/h = 250, k = 1, \Omega = 2450 \text{ rad/s}, m = 1, n = 6$)

When the excitation force is small, the deflection-velocity relation has the closed curve form as in Figs. 10 and 11.

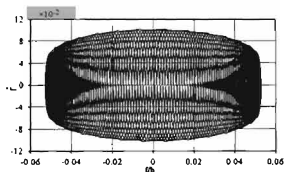


Fig. 10. Deflection-velocity curve of external stiffened cylindrical shell ($R/h = 250, k = 1, \Omega = 500 \text{ rad/s}, Q = 2 \times 10^5 \text{ N/m}^2, m = 1, n = 6$)

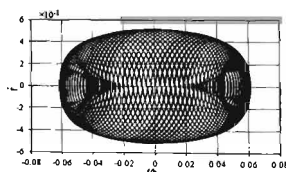


Fig. 11. Deflection-velocity curve of external stiffened cylindrical shell ($R/h = 250, k = 1, \Omega = 2450 \text{ rad/s}, Q = 2 \times 10^5 \text{ N/m}^2, m = 1, n = 6$)

When the excitation force increases, the deflection-velocity curve becomes more disorderly (see Figs. 12 and 13).

Figs. 14-16 present the effect of linear damping on nonlinear responses in with the linear damping coefficient $\mu = 0.3$. The damping lightly influences the response in the first vibration periods (Fig. 14). But, it considerably decreases the amplitude at the next far periods (Figs. 15 and 16).

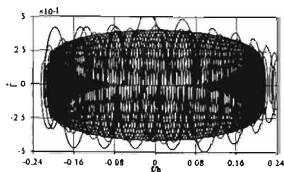


Fig. 12. Deflection-velocity curve of external stiffened FGM cylindrical shell ($R/h = 250$, $k = 1$, $\Omega = 500$ rad/s, $Q = 8 \times 10^5$ N/m², $m = 1$, $n = 6$)

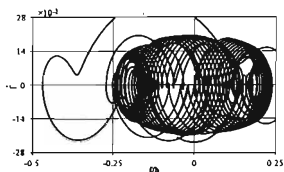


Fig. 13. Deflection-velocity curve of external stiffened FGM cylindrical shell ($R/h = 250$, $k = 1$, $\Omega = 2450$ rad/s, $Q = 8 \times 10^5$ N/m², $m = 1$, $n = 6$)

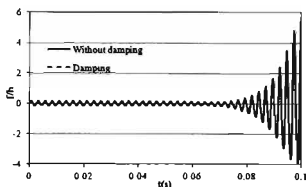


Fig. 14. Effect of damping on nonlinear responses of external stiffened FGM cylindrical shells ($R/h = 250$, $k = 1$, $\Omega = 2450$ rad/s, $Q = 5 \times 10^5$ N/m², $m = 1$, $n = 6$)

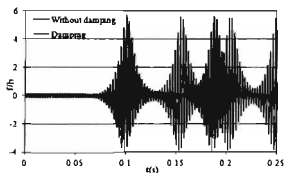


Fig. 15. Effect of damping on nonlinear responses of external stiffened FGM cylindrical shells ($R/h = 250$, $k = 1$, $\Omega = 2450$ rad/s, $Q = 5 \times 10^5$ N/m², $m = 1$, $n = 6$)

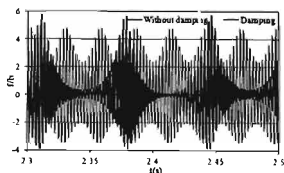


Fig. 16. Effect of damping on nonlinear responses of external stiffened FGM cylindrical shells ($R/h = 250$, $k = 1$, $\Omega = 2450$ rad/s, $Q = 5 \times 10^5$ N/m², $m = 1$, $n = 6$)

2.3. Nonlinear dynamic buckling of ES-FGM shell

Figs. 17-19 show the dynamic responses of un-stiffened and stiffened shells under mechanic load. The critical time t_{cr} can be taken as an intermediate value of instability region by according to the Budiansky-Roth criterion [5] and one can choose the inflexion point of curve i.e. $\left. \frac{d^2 f}{dt^2} \right|_{t=t_{cr}} = 0$ as Huang and Han [4].

Table 4. Dynamic critical buckling of FGM cylindrical shells under external pressure ($\times 10^5 \text{ N/m}^2$, $c = 10^6 \text{ N/m}^2\text{s}$)

k	Un-stiffened	Internal stiffeners	External stiffeners
$R/h = 125$			
0.2	12.506(7) ^d	44.520(6)	20.472(7)
1	8,038(7)	35.912(6)	16.535(7)
5	5,133(7)	27,067(5)	12.789(6)
10	4,576(7)	24.835(5)	11.670(6)
$R/h = 250$			
0.2	2.327(9)	26.484(6)	9.184(7)
1	1.568(9)	22.318(5)	8.338(7)
5	1,063(9)	16,335(5)	6.873(6)
10	0.992(9)	14.794(5)	6.387(6)

^d The numbers in the parenthesis denote the buckling modes $(n, m = 1)$.

Table 5. Dynamic critical buckling of FGM cylindrical shells under axial compression ($\bar{r}_0 = r_0 h$ ($\times 10^5 \text{ N/m}$, $c_r = 10^9 \text{ N/m}^2\text{s}$))

k	Un-stiffened	Internal stiffeners	External stiffeners
$R/h = 100$			
0.2	97.262(8,5) ^e	141.330(3,7)	116.860(4,9)
1	63.015(6,9)	100.618(3,7)	84.194(4,8)
5	37.910(6,8)	65.068(3,6)	56.914(4,8)
10	32.558(6,8)	56.728(3,6)	50.165(4,7)
$R/h = 250$			
0.2	15.631(12,10)	53.755(3,7)	35.896(5,10)
1	10.325(7,15)	41,135(3,7)	29.667(4,9)
5	6.280(6,13)	26.813(3,6)	22.180(4,8)
10	5.392(8,12)	23.401(3,6)	19.964(4,8)

^e The numbers in the parenthesis denote the buckling modes (m, n) .

Tabs. 4 and 5 show the critical dynamic buckling loads of stiffened and un-stiffened cylindrical shells under external pressure q_0 (Tab. 4) and under axial compression $\bar{r}_0 = r_0 h$ (Tab. 5) with four different values of $k = (0.2, 1, 5, 10)$. Clearly, the critical buckling load of stiffened shell is greater than one of un-stiffened shell. Tabs. 4 and 5 show that the critical dynamic load decreases with the increase of the volume fraction index k and the buckling modes (m, n) seem to be smaller for stiffened shells. Tabs. 4 and 5 also present the effect of R/h ratio on the critical dynamic buckling of shells. The critical dynamic buckling (external pressure and axial compression) of FGM cylindrical shell is strongly decreased when the R/h ratio increases.

Figs. 17 and 18 present effects of the loading speed on the dynamic responses of cylindrical shells under external pressure and axial compression with three values of loading speed. As can be seen, the critical dynamic buckling loads considerably increase when the loading speed increases.

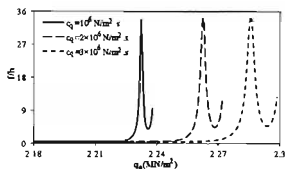


Fig. 17. Effect of loading speed on the dynamic responses of internal stiffened FGM shells under external pressure ($R/h = 250, k = 1, m = 1, n = 5$)

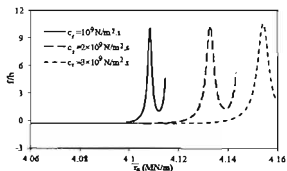


Fig. 18. Effect of loading speed on the dynamic responses of internal stiffened FGM shells under axial compression ($R/h = 250, k = 1, m = 3, n = 7$)

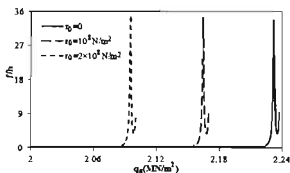


Fig. 19. Effect of pre-loaded compression on dynamic buckling internal stiffened FGM cylindrical shell ($R/h = 250, k = 1, m = 1, n = 5$)

Fig. 19 shows the dynamic response of stiffened circular cylindrical shell under combination of external pressure varying on time $q_0 = 10^6 t$ (N/m^2) and pre-loaded compressions $r_0 = \text{const}$. As can be observed, the pre-loaded compressions strongly influence on

the critical dynamic buckling of stiffened cylindrical shell. The critical dynamic buckling of shell decreases when the pre-loaded compression increases.

Table 6. Effects of stiffener position on the critical buckling of FGM cylindrical shells ($\times 10^5$)

	$q_0(\text{N/m}^2)$, $c = 10^6 \text{ N/m}^2\text{s}$		$\bar{r}_0(\text{N/m})$, $c = 10^9 \text{ N/m}^2\text{s}$	
	Static	Dynamic	Static	Dynamic
Un-stiffened	1.292(1,9) ^f	1.568(1,9)	9.995(7,15)	10.325(7,15)
External rings	7.654(1,7)	7.993(1,7)	10.401(15,1)	10.746(15,1)
Internal rings	21.504(1,5)	21.895(1,5)	10.368(13,8)	10.715(13,8)
External stringers	1.394(1,9)	1.686(1,9)	11.208(1,8)	11.508(1,8)
Internal stringers	1.302(1,9)	1.579(1,9)	10.446(1,8)	10.793(1,8)
External rings and stringers	7.994(1,7)	8.338(1,7)	29.316(4,9)	29.667(4,9)
Internal rings and stringers	21.923(1,5)	22.318(1,5)	40.701(3,7)	41.135(3,7)
External rings and internal stringers	7.816(1,7)	8.156(1,7)	32.898(2,8)	33.257(2,8)
Internal rings and external stringers	22.188(1,5)	22.587(1,5)	24.691(6,8)	25.096(6,8)

^f The numbers in the parenthesis denote the buckling modes (m, n).

The effect of type and position of stiffeners on the nonlinear critical buckling loads is given in Tab. 6. For FGM cylindrical shells under external pressure, the stringer stiffeners lightly influence and the ring stiffeners strongly influence to the critical buckling load of shells. Conversely, for FGM cylindrical shells under axial compression, the stringer stiffeners strongly influence and the ring stiffeners lightly influence to the critical buckling load of shells. Especially, the combination of ring and stringer stiffeners has a considerable effect on the stability of shells. Tab. 6 also shows that the critical dynamic buckling loads are greater than the critical static buckling loads of shells.

3. CONCLUSIONS

The nonlinear second-order differential three equations system (36-38) in Part 1 is solved by using the Runge-Kutta method and applying the Budiansky-Roth criterion to analyze the nonlinear dynamic response and critical dynamic buckling load. The frequency-amplitude relation of nonlinear vibration is also investigated. Some conclusions can be obtained:

- i). Harmonic beat phenomenon of a linear vibration is obtained when the excitation frequencies are near to natural frequencies.
- ii). Damping considerably influence on the amplitude of nonlinear vibration at the next far periods.
- iii). Stiffeners enhance the dynamic stability of cylindrical shells.
- iv). R/h ratio, position of stiffeners considerably influence on the nonlinear vibration and dynamic buckling of cylindrical shell.
- v). Stringer stiffeners lightly influence and the ring stiffeners considerably influence on the critical buckling load of shells for FGM cylindrical shells subjected to external

pressure. Conversely, the stringer stiffeners strongly influence and the ring stiffeners significantly influence on the critical buckling load of shells in the axial compression case.

ACKNOWLEDGMENT

This research is funded by Vietnam National Foundation for Science and Technology Development (NAFOSTED) under grant number 107.02-2013.02.

REFERENCES

- [1] D. H. Bich, D. V. Dung, and V. H. Nam. Nonlinear dynamical analysis of eccentrically stiffened functionally graded cylindrical panels. *Composite Structures*, **94**, (8), (2012), pp. 2465–2473
- [2] D. H. Bich, D. V. Dung, and V. H. Nam. Nonlinear dynamic analysis of eccentrically stiffened imperfect functionally graded doubly curved thin shallow shells. *Composite Structures*, **96**, (2013), pp. 384–395.
- [3] D. H. Bich, D. V. Dung, V. H. Nam, and N. T. Phuong. Nonlinear static and dynamic buckling analysis of imperfect eccentrically stiffened functionally graded circular cylindrical thin shells under axial compression. *International Journal of Mechanical Sciences*, **74**, (2013), pp. 190–200.
- [4] H. Huang and Q. Han. Nonlinear dynamic buckling of functionally graded cylindrical shells subjected to time-dependent axial load. *Composite Structures*, **92**, (2), (2010), pp. 593–598.
- [5] B. Budiansky and R. S. Roth. Axisymmetric dynamic buckling of clamped shallow spherical shells. *NASA Technical note D-510*, (1962).
- [6] J. L. Sewall and E. C. Naumann. An experimental and analytical vibration study of thin cylindrical shells with and without longitudinal stiffeners. *NASA Technical note D-4705*, (1968).
- [7] J. L. Sewall, R. R. Clary, and S. A. Leadbetter. An experimental and analytical vibration study of a ring-stiffened cylindrical shell structure with various support conditions. *NASA Technical note D-2398*, (1964).
- [8] M. Baruch and J. Singer. Effect of eccentricity of stiffeners on the general instability of stiffened cylindrical shells under hydrostatic pressure. *Journal of Mechanical Engineering Science*, **5**, (1), (1963), pp. 23–27.
- [9] J. N. Reddy and J. H. Starnes. General buckling of stiffened circular cylindrical shells according to a layerwise theory. *Computers & Structures*, **49**, (4), (1993), pp. 605–616.
- [10] H. S. Shen. Postbuckling analysis of imperfect stiffened laminated cylindrical shells under combined external pressure and thermal loading. *International Journal of Mechanical Sciences*, **40**, (4), (1998), pp. 339–355.